Fuel 238 (2019) 98–110

Contents lists available at ScienceDirect

Fuel

journal homepage: www.elsevier.com/locate/fuel

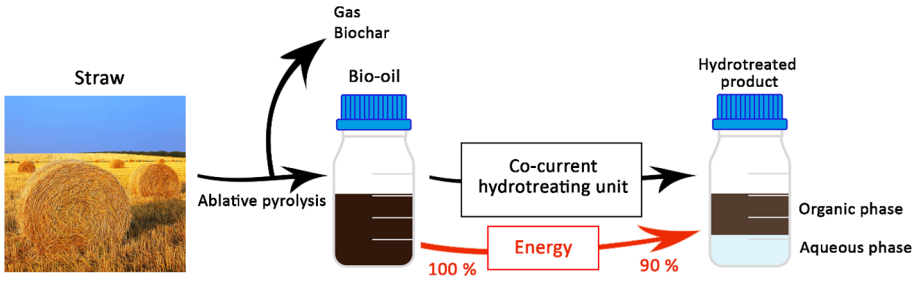
Full Length Article

Hydrotreatment of straw bio-oil from ablative fast pyrolysis to produce suitable refinery intermediates

Miloš Auersvald, Bogdan Shumeiko, Dan Vrtiška, Petr Straka, Martin Staš, Pavel Šimáček, Josef Blažek, David Kubička*

University of Chemistry and Technology Prague, Department of Petroleum Technology and Alternative Fuels, Technická 5, 166 28 Prague, Czech Republic

GRAPHICAL ABSTRACT



ARTICLE INFO

Keywords:
Hydrotreatment
Straw bio-oil
Ablative fast pyrolysis (AFP)
Biofuels
Sulphided catalysts

ABSTRACT

To meet the expected requirements of the proposed EU Renewable Energy Directive for the next decade (RED II), it is necessary to increase the availability of second-generation biofuels. One promising way of doing this involves using ablative fast pyrolysis units to transform an agricultural by-product, for example straw, into bio-oil. To obtain straw bio-oil suitable for processing in a typical refinery, we optimized the key parameters of its hydrotreatment. For the upgrading, a continuous flow reactor with a fixed bed of a commercial sulphide NiMo/Al_2O_3 catalyst was used. The reaction temperature and pressure were tested at 240–360 °C and 2–8 MPa, respectively. The reaction off-gas was analysed by GC-FID/TCD. A detailed physicochemical analysis of the products was carried out. Under most conditions tested, the product was separated into an aqueous and an organic phase. For the best products, > 85% of the feed energy content remained in the organic phase and a significant decrease in viscosity and acidity was achieved. The product prepared at 360 °C and 8 MPa was the only one completely miscible with straight-run gas oil and, thus, appears to be the most suitable for co-processing in a refinery.

1. Introduction

Fossil fuels are currently used to cover about 78% of our global energy demand [1]. Their reserves are, however, finite and their use has adverse environmental impacts as their combustion contributes to a gradual increase in CO_2 concentration in the atmosphere. Apart from CO_2 itself, biomass is the only renewable feedstock containing carbon that can be converted to liquid fuels [2]. Considering the ever-growing human population and the associated growing demand for food and water, it follows that a further increase in the production of the first-generation biofuels is not sustainable and thus not acceptable. Consequently, the EU Commission proposal for the new EU Directive (RED II)

* Corresponding author.
E-mail address: david.kubicka@vscht.cz (D. Kubička).

https://doi.org/10.1016/j.fuel.2018.10.090
Received 25 June 2018; Received in revised form 4 October 2018; Accepted 15 October 2018
Available online 24 October 2018
0016-2361/ © 2018 The Author(s). Published by Elsevier Ltd. This is an open access article under the CC BY-NC-ND license (http://creativecommons.org/licenses/BY-NC-ND/4.0/).

demands a decrease in the food-based biofuels from 7% (energy content) in 2021 down to 3.8% by 2030. In addition, the EU COM draft for RED II proposes a sub-target of 3.6% (energy content) blending for advanced biofuels originating from residues either directly from agriculture or indirectly as a by-product from food/feed production. An example of acceptable feedstock for advanced biofuels production is lignocellulosic biomass, such as straw, also listed in Annex IX of the drafted EU directive [3]. The final RED II directive is expected to be available in Q3 or Q4 of 2018 and is currently getting developed in a joint consultation ("trilogue") between EU Commission, EU Council and EU Parliament.

A variety of biomass-upgrading technologies was investigated, such as pyrolysis, gasification, hydrothermal upgrading, depolymerisation, *etc.* [4]. Among them, pyrolysis stands out as one of the few biofuel technologies that can handle a range of biomass feedstocks (agri-residues, forest residues, energy crops, municipal solid wastes). Hence, it is an attractive option for expanding the biomass availability by using less desirable biomass. In this context, ablative fast pyrolysis (AFP) is of particular interest as it does not require reducing the particle size of biomass, which is a significant advantage over fluidized bed pyrolysis requiring energy-intensive grinding when it comes to straw pyrolysis [5]. Also, the possible mobility of AFP unit would be beneficial for straw upgrading as it would allow avoiding the inefficient transport of straw biomass over long distances (80% of straw cost are logistic cost) [5]. Finally, AFP is also characterized by low construction and operational costs [6].

From the liquid biofuels point of view, the key product of pyrolysis is the liquid called bio-oil or pyrolysis oil whose yield is typically up to 75 wt% [7]. The yields of by-products, *i.e.* gases and char, are typically 13 and 12 wt%, respectively [7]. An efficient use of these by-products, *i.e.* gases to heat, *e.g.* the spinning hot rotor of the pyrolysis device and char for rejuvenation of tired soils, also reduce the bio-oil production prices [8]. Thanks to its composition, bio-oil could become one of the alternative sources of renewable energy which could provide liquid biofuels in future. However, crude bio-oil has due to its high oxygen content and degree of unsaturation some undesirable properties such as (i) low thermal and oxidation stability, (ii) high acidity and thus high corrosiveness and (iii) immiscibility with non-polar petroleum fractions. These properties prevent direct upgrading of bio-oils in refineries and appropriate upgrading (stabilization) of bio-oil is necessary prior to its upgrading or co-processing in a conventional refinery.

The possible co-processing of partially upgraded bio-oils seems especially advantageous in a situation when there are overcapacities in the EU refining sector [9] as it would promote employment in the sector and its further development while securing second-generation biofuels. When considering available refinery processes for bio-oil co-processing, hydrotreatment appears to be more beneficial than catalytic cracking as it affords higher yields and better quality of the upgraded product. This is a consequence of deeper deoxygenation and suppressed formation of gaseous and solid by-products [10]. In addition, refinery overcapacities could also be used for the primary bio-oil upgrading (stabilization) by their revamping to satisfy (meet) the specific requirements of bio-oil treatment.

Numerous detailed studies [11–14] deal with a wide variety of catalysts and process conditions for hydrotreatment/deoxygenation of lignocellulosic bio-oils to fuels and other valuable products. With respect to their active phase, the catalysts for bio-oil hydrotreatment can be divided into the following groups: (i) noble metals, (ii) transition metals and (iii) metal sulphides. Many of them are used in crude oil refining processes [15].

Among noble metals, mainly Pt, Pd, Ru and Rh were tested for bio-oil upgrading [11,16,17]. They have shown outstanding results in the conversion of oxygen-containing compounds present in bio-oils [18–20]. Unfortunately, their very high hydrogenation activity leads to increased hydrogen consumption and operating costs [21,22]. Another disadvantage of noble metal catalysts is that they can be poisoned by even small contents of sulphur present in lignocellulosic bio-oils. Due to the high acidity and water content in bio-oils, carbon supports that would not deteriorate too fast like, *e.g.* alumina supports have attracted considerable attention [23].

Transition metals have been studied as a possible alternative, the focus being on Ni, Mo, Co, Fe and Cu based catalysts [24,25] due to their good catalytic performance. In addition to metallic catalysts also phosphides, carbides and nitrides of transition metals have been investigated [13,14,26,27]. Zhao et al. [28] found that metal phosphide catalysts were more active in deoxygenation than the traditional $CoMoS/Al_2O_3$ and the commercial 5% Pd/Al_2O_3 catalysts.

Despite the promising performance of metallic catalysts, the sulphided catalysts, predominantly alumina-supported NiMo and CoMo catalysts, remain the preferred choice for bio-oil hydrotreatment thanks to being well-established and robust [29]. Their performance has been reviewed extensively by Patel et al. [30] and Mortensen et al. [10]. A wide range of experimental conditions have been covered in studies using sulphided catalysts in hydrotreatment of bio-oils originating from different feedstocks, but straw. Temperature and hydrogen pressure were varied between 200 and 450 °C and 1–29 MPa, respectively [23,25,31,32]. Due to the thermal instability of bio-oils, two-stage upgrading was often applied [11,23] with mild conditions in the first stage to remove the most reactive compounds and with more severe conditions in the second stage to eliminate recalcitrant oxygenates. The sulphur content of bio-oils is, compared to petroleum fractions, low, typically several hundred ppm [21,30]. Consequently, sulphided catalysts tend to lose their activity during hydrotreatment of bio-oils, unless a source of H_2S is added to protect the active sulphided phase of the catalyst from reduction [33]. The effects of H_2S and water on the deoxygenation of carbonyl, carboxylic, and guaiacyl groups over alumina-supported sulphided NiMo/CoMo catalysts were studied by Laurent et al. [34]. They concluded that H_2S increased the Bronsted acidity of the catalysts which promoted decarboxylation reactions, but it suppressed the deoxygenation of the carbonyl groups [34].

Nonetheless, sulphided catalysts showed good activity and selectivity in bio-oil hydrotreating [12,35] and if the stabilized (partially deoxygenated) bio-oil would be further upgraded in a refinery, the slightly increased sulphur content in comparison with the raw bio-oil would not cause any problems. Commercial hydrotreating catalysts (sulphided NiMo and CoMo) were investigated in a three-heating-zone reactor (170–250, 250–350, 350–450 °C) for converting a wood-derived bio-oil into renewable hydrocarbons by Horáček et al. [36]. The alumina-supported sulphided CoMo catalyst showed better selectivity to diesel-like products and deeper hydrogenation of gaseous intermediates (CO_x) than the sulphided NiMo catalyst. In contrast, the sulphided NiMo catalyst was found to be more active in decarboxylation and it was possible to reach a steady state production of hydrocarbons having a comparable boiling point distribution as petroleum-derived middle distillates [36]. However, the catalysts suffered from low stability of the alumina support material at high temperatures in the presence of water [33]. Similarly, Gholizadeh et al. [35] reported hydrotreating of palm bio-oil in a fixed bed flow reactor over $NiMo/Al_2O_3$ catalyst at 7 MPa hydrogen pressure and 370–450 °C. When increasing the temperature, the oxygen content in the upgraded product was reduced below 2 wt% [35].

Despite being a valuable sustainable renewable feedstock that could be abundantly available in the Europe, upgrading of bio-oil obtained from ablative fast pyrolysis of wheat/barley straw by its hydrotreatment has received only very little attention so far. Therefore, we report here the effect of key reaction parameters on the yields and properties of the hydrotreated products originating from straw bio-oil from ablative fast pyrolysis with the aim to obtain a product upgradeable in a conventional refinery rather than a fully-deoxygenated product. To the best of our knowledge, this has not been attempted in the previous studies. In addition, we propose for the first time the use of principal component analysis (PCA) classification of products to assess the degree

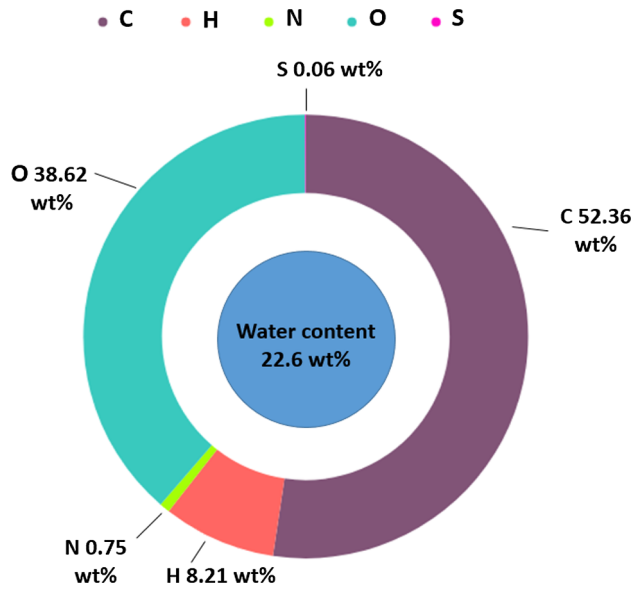


Fig. 1. Elemental composition and water content in bio-oil.

of deoxygenation of hydrotreated bio-oils allowing real time analysis of products and adjustment of reaction conditions.

2. Experimental

2.1. Materials

Straw bio-oil was produced at Fraunhofer UMSICHT by ablative fast pyrolysis of straw (wheat and barley straw, 1:1 w/w). The straw pellets were pressed onto a hot rotating disc and pyrolyzed at 550 °C with vapour residence time less than 1 s. After condensation at 2–5 °C, the liquid product spontaneously separated into an aqueous and an organic phase (bio-oil). For more details, see [37]. The bio-oil was filtered to remove any residual solids, doped with dimethyl disulphide (DMDS, ≥99.0%) supplied by Sigma-Aldrich to contain 0.5 wt% of DMDS to maintain the catalyst activity and used in the experiments. The basic properties of the straw bio-oil are summarized in Fig. 1 and Table 1. A conventional commercial sulphided $NiMo/Al_2O_3$ catalyst (5.5 wt% NiO and 28.3 wt% MoO_3) and hydrogen (99.9 vol%) supplied by SIAD (Czech Republic) were used in the experiments.

2.2. Bio-oil hydrotreating

Bio-oil was hydrotreated in an electrically heated fixed bed reactor (inner diameter 23 mm) having a thermo-well (outer diameter 4 mm) in its axis with 10 thermocouples. The reactor was loaded with 55 g of a NiMo catalyst. The catalyst particle sizes 0.25–0.42 in lower part and 0.85–1.5 mm in upper part of reactor were used. A metallic preheater was placed above the catalyst bed. Prior to the experiments, the catalyst was *in-situ* sulphided at 345 °C and 4 MPa using a mixture of hydrotreated gas oil and DMDS containing 3.8 wt% DMDS. The catalyst activation was followed by its stabilization using straight-run gas oil (0.23 wt% S) for 24 h at 340 °C, 4 MPa and WHSV ca $1 \cdot h^{-1}$. Then, the temperature in the reactor was adjusted to the first tested temperature (240 °C) and bio-oil feeding in the reactor was started. The experiments were carried out at WHSV of approximately $1\ h^{-1}$ and hydrogen flow-rate of $90\ l \cdot h^{-1}$. The reaction temperature and pressure were varied in the range 240–360 °C and 2–8 MPa, respectively. Liquid samples were collected for 2 h at each reaction condition from the moment when all reaction parameters were stabilized. Water phase was separated from organic phase that was analysed as described below by an array of analytical methods. During of each sampling period, the reaction off-gas was also collected into a sampling bag and analysed by GC-FID/TCD. An overview of the experimental reaction conditions, products samples and corresponding times on stream is given in Results and Discussion section (Table 2).

Table 1
The properties of the bio-oil.

Parameter	Value
Density at 15 °C [$g \cdot cm^{-3}$]	1.13
Kinematic viscosity at 40 °C [$mm^2 \cdot s^{-1}$]	140
Higher heating value [$MJ \cdot kg^{-1}$]	23.3
Lower heating value [$MJ \cdot kg^{-1}$]	21.5
Total acid number [mg $KOH \cdot g^{-1}$]	98.9
Carboxylic acid number [mg $KOH \cdot g^{-1}$]	54.3
Micro Conradson residue [wt%]	15

Table 2
An overview of experimental conditions, product samples and times on streams (TOS).

Sample	Average temperature in catalytic zone [°C]	TOS [h]	Sample	Average temperature in catalytic zone [°C]	TOS [h]
240/4	242	19	300/2	298	45
260/4	261	23	320/2	320	69
280/4	280	29	340/2	341	60
300/4	300	36	300/4	297	36
320/4	315	42	320/4	318	26
340/4	338	74	340/4	339	31
360/4	358	81	300/8	297	11
			320/8	319	7
			340/8	339	21
			360/8	361	52

2.3. Analyses of feed and products

Elemental composition (C, H, N, S) was determined using a Vario EL Cube analyser (Elementar). A Merck stearic acid standard and a standard by Elementar Analysensysteme GmbH (C: 67.68 wt%, H: 4.95 wt%, N: 0.69 wt%, S: 0.81 wt%) were used for the instrument calibration. The sample (5–15 mg) was burned in a pure oxygen atmosphere. Gaseous combustion products were separated after reduction in a purge and trap chromatographic system and finally detected by a thermal conductivity detector (TCD). The oxygen content was calculated by difference.

The water content was determined by a Karl Fischer volumetric titration according to the ASTM E203 using a METTLER TOLEDO DL38 device. A small amount of sample (0.02–0.05 g) was injected into a glass chamber containing HYDRANAL™-KetoSolver (Karl Fischer solvent, Honeywell). Titration was carried out by Karl Fischer titrant Composite 5 K (Riedel-de Haën).

Density at 15 °C and kinematic viscosity at 40 °C were determined by an SVM 3000 Stabinger Viscometer (Anton Paar). Micro Conradson carbon residue (MCR) was determined according to the ASTM D4530 standard method, by an NMC 420 device (NORMALAB ANALIS).

The higher heating value (HHV) was determined by an IKA 2000 device (Merci). Sample (0.5–1.0 g) was weighed into a crucible for reaching an ideal temperature increase of $3–5\ °C \cdot min^{-1}$. The lower heating value (LHV) was calculated from the HHV reduced by the evaporation heat of the water in the sample and the water produced by the combustion of hydrogen.

Total acid number (TAN) and carboxylic acid number (CAN) were determined by a 716 DMS Titrino instrument (Metrohm AG). TAN was determined according to the ASTM D664, with KOH as a titrant, LiCl as an electrolyte and a mixture of toluene:isopropanol:water (100:99:1 V/V) as a solvent were used. CAN was determined by a titration method

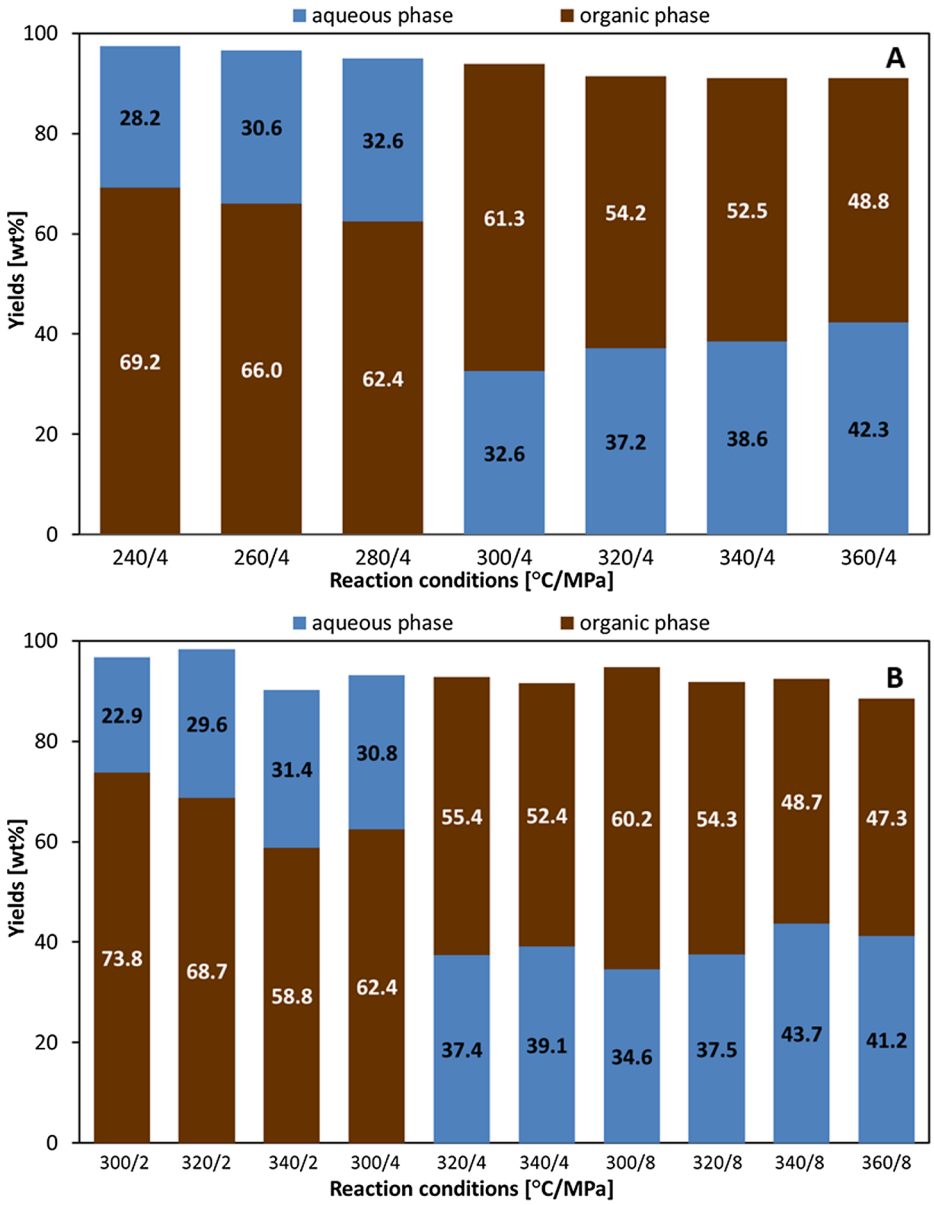


Fig. 2. Yields of organic and aqueous phases under different reaction temperatures at pressures (A) 4 MPa and (B) 2; 4 and 8 MPa.

[38], with tetrabutyl ammonium hydroxide as a titrant, tetraethyl ammonium bromide as an electrolyte, and isopropanol as a solvent were used.

Bio-oil and all liquid organic products were characterized by simulated distillation. Samples were dissolved in carbon disulphide (1 wt % solution) and introduced to a TRACE ULTRA gas chromatograph (Thermo Scientific) equipped with an on-column injector, Agilent J&W CP-SimDist UltiMetal (10 m × 0.53 mm × 0.17 μm) column, an FID detector and an oven cryogenic cooling system. The absolute accuracy of the simulated distillation was negatively affected by the presence of oxygenates in the samples, and thus a "recovery" parameter was calculated from the concentration and total chromatogram area for all samples to allow a comparison of samples. This parameter expresses the percentage of sample response related to the response of completely eluted hydrocarbons, which have, *per definition*, the "recovery" parameter equal to 100%.

All liquid samples (both organic and aqueous phases) were characterized by FTIR-ATR (Attenuated Total Reflection) technique. An infrared spectrometer IRAffinity-1 (Shimadzu, Japan) with Quest ATR accessory with a diamond crystal (Specac, USA) was used to record the FTIR spectra. LabSolution IR software (Shimadzu, Japan) was used as an interface between the spectrometer and the control computer. The spectra were recorded in the 4000–650 cm^{-1} region using the spectral resolution of 4 cm^{-1} and 128 scans.

Due to the complexity of the spectra, principal component analysis (PCA) was employed as a tool allowing a direct comparison of individual samples. PCA is a method used for a reduction of usually large data sets [39]. The original variables (*e.g.* spectroscopic data) are replaced by new variables called principal components (PCs) which are linear combinations of the original variables. The new variables are mutually orthogonal and uncorrelated. The first few principal components usually explain most of the relevant variability of the original dataset. Each sample gets its own set of values (scores) for each principal component, so it is possible to create plots of the score values and compare the samples based on their position in the plots.

Two analytical methods were used for analysis of gaseous products collected in 10 L Tedlar sampling bags: (i) determination of permanent gases and lighter hydrocarbons and (ii) determination of higher hydrocarbons and other organic compounds. The determination of permanent gases (H_2, CO, and CO_2) and light hydrocarbons and oxygenates

(C_1–C_5) was performed using a Hewlett Packard HP 6890 gas chromatograph equipped with a CP-Carbobond fused silica column (50 m × 0.53 mm × 5 μm) and two detectors; a flame ionization detector (FID) for detection of the hydrocarbons (C_1–C_5) and a thermal conductivity detector (TCD) for detection of the permanent gases. The effluent flowing out of the column was split into the detectors using a Y-piece Siltek MXT Connector (Restek). The content of higher hydrocarbons and other organic compounds was determined using an Agilent 6890 gas chromatograph equipped with an HP-PONA column (50 m × 0.2 mm × 0.5 μm) and an FID detector. Major higher hydrocarbons and other selected organic compounds were identified based on the retention times of pure substances and previous GC–MS analysis of biooil. The content of "other organic substances" including oxygenates and C_{6+} hydrocarbons was expressed as a sum using an estimated response factor of 1.2.

3. Results and discussion

3.1. Experiments performed

Two sets of experiments were performed, each with fresh catalyst at the beginning of the experiment. The first set was performed at a pressure of 4 MPa, the second set at pressures 2, 4 and 8 MPa. An overview of experimental conditions, designation of the gained product and times on stream in which they were obtained is listed in Table 2.

3.2. Mass and energy balance

The yields of liquids from bio-oil hydrotreating exceeded 90 wt% in the full range of experimental conditions (Fig. 2A and B), except product obtained at 360 °C and 8 MPa, where it attained 88.5 wt%. When considering the yield of gaseous products, the mass balance was almost completely closed. The observed slight differences in mass balance can be attributed mainly to losses during manipulation with samples and to a much smaller extent due to the formation of carbonaceous deposits on catalyst.

Reaction temperature had a pronounced effect on the yield of aqueous and organic phase. Under mild temperatures (< 300 °C), the yield of the aqueous phase was < 33 wt% (Fig. 2A), which indicates a low degree of deoxygenation (taking into account that water present in bio-oil was 22.6 wt%). As a result of (partial) deoxygenation especially at higher temperatures (> 300 °C), the yield of organic phase decreased, and its density became lower. Consequently, the order of the phases changed as indicated in Fig. 2A. At the same time, the yield of aqueous phase increased up to ca. 42 wt%.

Similarly, hydrogen pressure affected the yields of both liquid phases as well. The deoxygenation degree was lower at lower hydrogen pressures (particularly at 2 MPa) and hence less aqueous phase was formed and separated. Due to the higher density of the organic phase at these conditions, the aqueous phase was the top layer. A comparison between Fig. 2A and B reveals that the yields of liquid phases obtained at 340 °C and 4 MPa were similar in both tests despite the different time-on-stream (TOS), at which these samples were collected (TOS: 74 h in Fig. 2A and 31 h in Fig. 2B), and of different history of the catalysts. The yields of the organic and aqueous phases as a function of the hydrotreating severity demonstrate that the yields of gaseous phases (typically 2–10 wt%) increased slightly with the increased hydrotreating severity. However, extensive cracking was not observed (as discussed below).

In addition to maximizing the mass yield of the liquid organic fraction suitable for further refinery upgrading into fuel components, it is critical to ensure that most of the energy contained in the bio-oil feed is kept in the liquid organic phase. The share of the initial energy content that is transferred in the organic liquid phase, *i.e.* the energy content of the organic phase divided by the energy content of the fed bio-oil multiplied by the yield of this phase and by 100 is denoted as "energy recovery" (based on lower heating value) and reported in Fig. 3 as a function of reaction conditions. The values above 100 (Fig. 3B) thus indicate that more energy was incorporated in the liquid organic products than lost to other product streams. Specifically, hydrogenation of unsaturated bonds and reduction of aldehydes and ketones to corresponding alcohols were the main reactions at mild reaction conditions, while deoxygenation and hydrogenolysis reactions occurred mainly at more severe conditions (> 320 °C and pressures 4 or 8 MPa). Due to these reactions, some of the energy was lost from the organic liquid phase to the gas phase and the energy carried in by hydrogen was lost as water. Nonetheless, it is positive that > 85% of the initial energy content of bio-oil can be kept in the organic liquid phase, *i.e.* in the targeted product.

4. Liquid products

4.1. Composition

The composition of hydrotreated products changes gradually and reflects well the changes in the experimental conditions. At 300 °C and 2 MPa, some of the reactive groups, such as double bonds and carbonyls, were saturated, and deoxygenation, *e.g.* by dehydration, decarbonylation or decarboxylation took place although it was not very significant. This explains also the observed increase in the energy recovery to values > 100% (Fig. 3) and is as well reflected in the calculated degree of deoxygenation (DOD, a difference of the organically-bound oxygen in bio-oil and products divided by the organically-bound oxygen in bio-oil). An increase in the reaction temperature (from 240 to 360 °C) led to a continuous increase in the H/C atomic ratio and at the same time a significant decrease in the O/C atomic ratio (from ca. 0.18 to about 0.04, Fig. 4A). This confirms that in this temperature range deoxygenation reactions accompanied by hydrogenation reactions, *e.g.* saturation of double bonds after dehydration, took place. These trends were the same also in the full range of hydrogen pressure (2–8 MPa). In addition, it is also obvious that the increase in the hydrogen pressure promoted hydrogenation reactions, as indicated by the increase in the H/C atomic ratio from ca. 1.4 at 320–340 °C and 2 MPa to ca. 1.6 at 320–340 °C and 8 MPa (Fig. 4B). At the same time, deoxygenation reactions were promoted as well since for a constant temperature, *e.g.* 320 or 340 °C, there was a significant drop in the O/C atomic ratio (Fig. 4B) when hydrogen pressure was increased.

Raw bio-oils, as well as products of their hydrotreating, are very complex mixtures of many compounds, which render the analysis of their composition very difficult. Nonetheless, it is important to extract at least qualitative information about the composition in "real time" to steer the conversion process efficiently, *i.e.* to adapt reaction parameters to compensate the loss of catalyst activity and to maintain product quality. Therefore, we propose two methods, one chromatographic and one spectroscopic that enable a quick characterization of the obtained products.

The chromatographic method is based on the simulated distillation (SIMDIS) analysis. Applied to bio-oils and products of their hydrotreating, it allows estimating the "hydrocarbon-likeliness" of the product and its approximate fractional composition. The analysis relies on the different response factor of hydrocarbons (here by definition set to 100%) and that of the oxygenates which is always lower, nonetheless related to the oxygen content of the compounds. As shown in Fig. 5A, already hydrotreating at 240 °C resulted in an increase in the SIMDIS recovery from 32 to 42%. The data further evidence that deoxygenation extent increases with the increasing reaction temperature. It has to be noted that the data are reported yields related to the feed, *i.e.* the sum of the yields is less than 100% due to formation of water and gases. The fractional composition suggests (Fig. 5B) that majority of the products is within the diesel fuel range (about 30%, which corresponds to ca. 50% of the fractions). Interestingly, the amount of the heaviest products increased from 8% determined in the feed to 16% found in the products

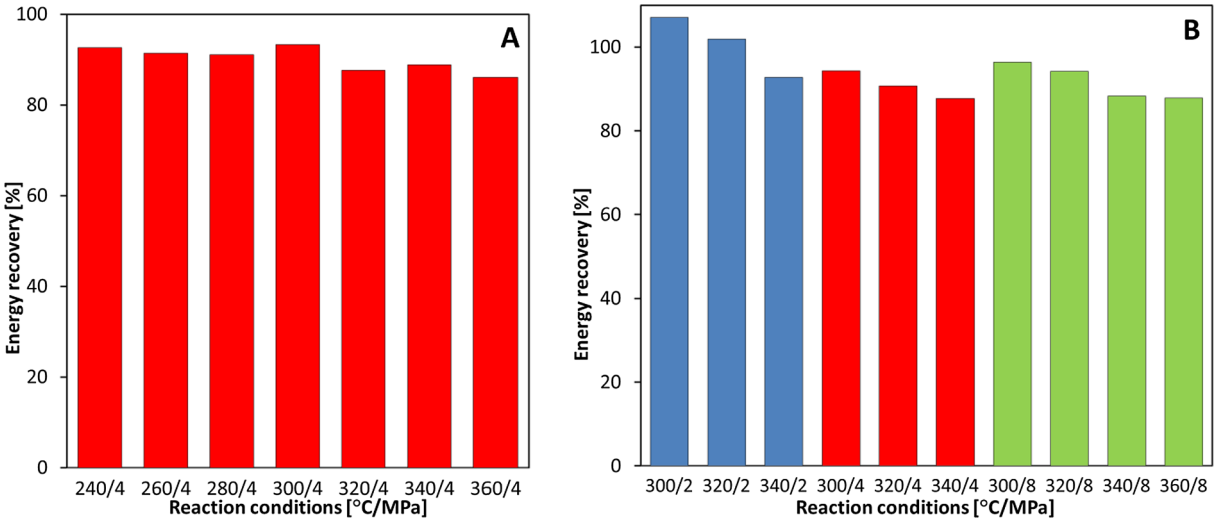


Fig. 3. Energy recovery at different reaction conditions (A) 4 MPa and (B) 2; 4 and 8 MPa.

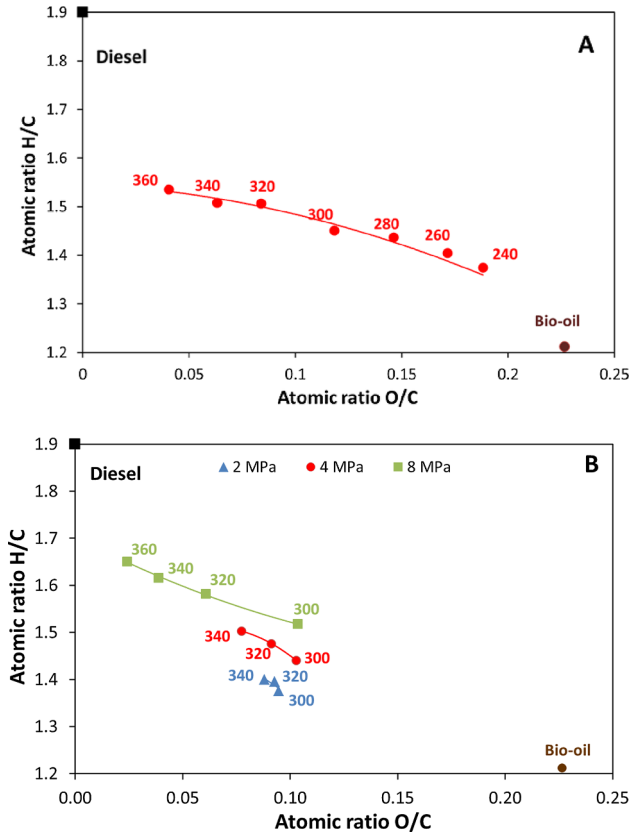


Fig. 4. Van Krevelen diagram of diesel fuel, feed bio-oil and hydrogenated products under different reaction temperatures at pressure (A) 4 MPa and (B) 2; 4 and 8 MPa.

at 280 °C. This significant increase (Fig. 5B) cannot be explained simply by the formation of gaseous products due to deoxygenation of short-chain oxygenates and has to be attributed to the occurrence of condensation reactions. However, further increase in reaction temperature resulted in a dramatic reduction of the heaviest products down to 5% at 360 °C (Fig. 5B) due to significant deoxygenation as evidenced by the increasing SIMDIS recovery (Fig. 5A) and the calculated deoxygenation degree (Fig. 8C). At the same time, the yields of gasoline- and diesel-like fractions increased (Fig. 5B) together with the increasing yield of gaseous products (Fig. 10A).

The effects of both reaction temperature and pressure on the SIMDIS recovery are presented in

Fig. 5C. As expected, both parameters have a positive effect, although the increase in SIMDIS recovery when increasing hydrogen pressure from 4 to 8 MPa is rather modest, especially at lower temperatures. Interestingly, the combination of high temperature and pressure (360 °C and 8 MPa) resulted in almost complete deoxygenation and the SIMDIS recovery reached 96%, *i.e.* the product consisted almost exclusively of hydrocarbons (Fig. 5C). The effect of pressure on the fractional composition is demonstrated in Fig. 5d. In line with the effects described for reaction temperature, the more severe reaction conditions promoted (hydro) cracking reactions affording thus more gasoline-like products and less heavy products. Also, at lower hydrogen pressure it could be confirmed that condensation reactions resulting in the formation of heavier products took place and their yield increased from 8% found in bio-oil to ca. 12% formed in the products obtained at 2 MPa and 340 °C (Fig. 5D).

4.2. FTIR spectra and principal component analysis

A complementary method for rapid screening of the character of bio-oil and products of its hydrotreating (in terms of composition) was based on FTIR.

As seen in Fig. 6, the spectra are rather complex and the changes are only subtle to allow elucidating in detail the changes in composition.

Fig. 6A shows the entire spectrum of the bio-oil and the spectra of selected products obtained by bio-oil hydrotreating. To analyse the changes, three spectral regions (B, C and D) containing the most important spectral features have been displayed in Fig. 6B–D and will be discussed separately. The broad band occurring in the region of approximately 3700–3000 cm^{-1} (Fig. 6B) can be attributed to the stretching of the OH group, which is typical for alcohols, phenols, carboxylic acids and water [40]. Signal intensity of this band in all products spectra was lower than in the feed spectrum. Moreover, the increase in the reaction temperature and pressure always led to a decrease in the signal intensity of the OH band. It can be mainly attributed to the water content decrease which was confirmed using KF titration (Figs. 8C and 9D). Nevertheless, a decrease in other OH group-containing compounds, whose other absorption bands can be found in the region 1300–1000 cm^{-1}, was observed as well. On the other hand, the bands in the region 3000–2800 cm^{-1} (Fig. 6B), which can be attributed to the asymmetrical and symmetrical stretching of the C–H bonds originating from the methyl and methylene groups, were stronger in the products spectra. As expected, the highest signal intensity of these

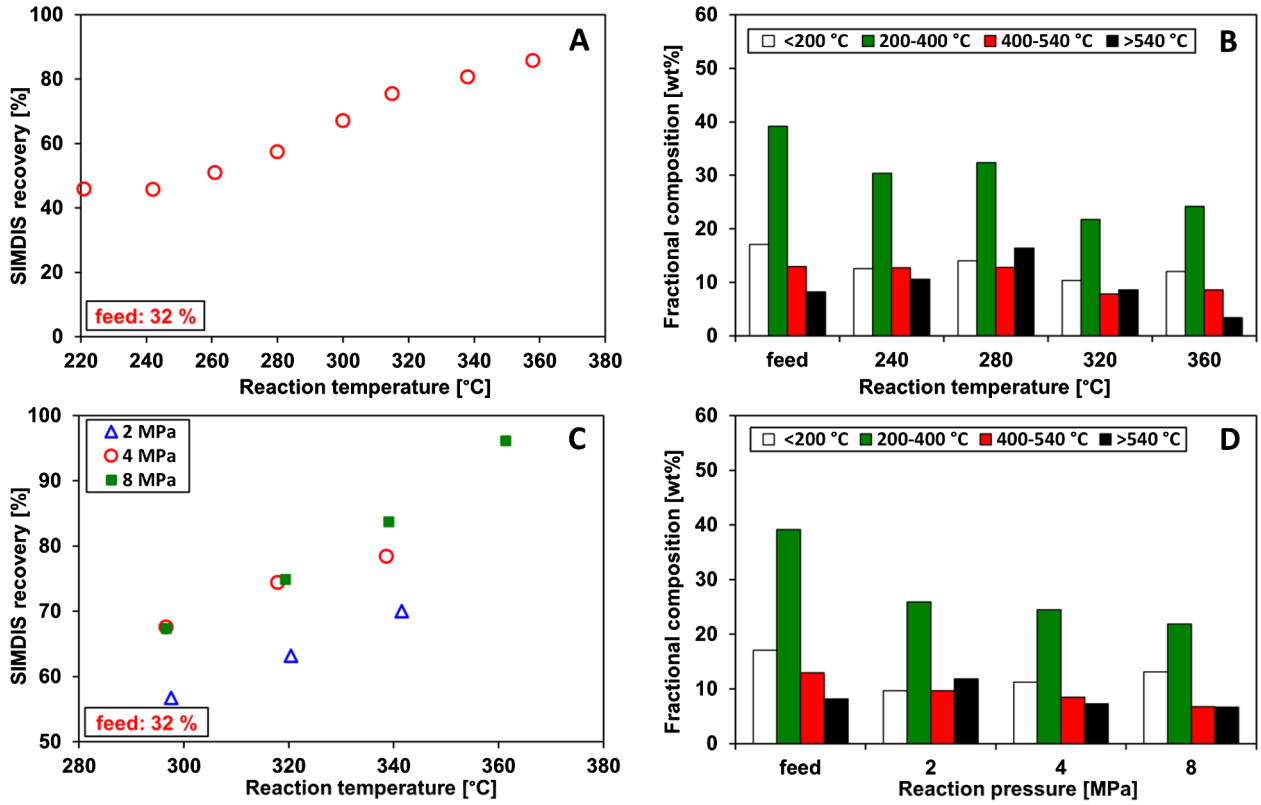


Fig. 5. SIMDIS recovery as a function of reaction temperature at 4 MPa (A), yield of fractions (on water-free basis) obtained at different temperatures at 4 MPa (B), SIMDIS recovery as a function of reaction temperature at different pressures (C) and yield of fractions (on water-free basis) obtained at 340 °C at 2–8 MPa (D).

bands was observed in the spectrum of the product obtained at the most severe conditions.

The spectral region 1820–1320 cm^{-1} (Fig. 6C) consists of signals belonging to the stretching of the C═O groups and the stretching of the C═C bonds from aromatics or alkenes. Moreover, scissoring vibration of water molecule occurs in this region. An evident change in the absorption intensity of the feed and products can be seen. Most importantly, the band with the maximum signal intensity at 1697 cm^{-1}, which can be attributed to the C═O groups (*e.g.*, ketones, aldehydes and carboxylic acids), was eliminated at the most severe reaction conditions. The intensity of the bands in the region 1630–1570 cm^{-1} and at 1514 cm^{-1} belonging to the stretching of the C═C bonds in aromatics (*e.g.*, phenols) decreased as well.

The spectra of the spectral region 1320–650 cm^{-1} are shown in Fig. 6D. The overlapped bands in the 1320–1000 cm^{-1} region can be attributed to the oxygen-containing groups present for example in phenolic compounds with hydroxyl and methoxy groups, aldehydes, carboxylic acids, glycosides, *etc.* It should be noted that the content of these compounds decreased with the increasing severity of reaction conditions. Moreover, some bands (*e.g.*, alkyl-aryl ethers and glycosides) disappeared almost completely when the highest temperature was applied. The bands in the 900–650 cm^{-1} region can be mainly attributed to the out-of-plane deformation vibrations of aromatic ═C−H groups. Besides these bands, the out-of-plane deformation of O−H groups of phenols occurs in this region. Signal intensities in this region are strongly influenced by the broad band caused by deformation vibrations of water.

Although significant changes in the FTIR-ATR spectra can be observed upon careful visual inspection of the spectra, only qualitative conclusions can be drawn. Thus, to extract more valuable information and to enable a comparison of individual products, principal component analysis (PCA) of the spectra was applied. In addition to the spectra of the bio-oil hydrotreating products, *i.e.*, organic and aqueous phases, and the feed, *i.e.*, bio-oil, a spectrum of water and spectra of other batches of straw bio-oil were added to the data set. The first two principal components (PC1 and PC2) captured 99.4% of the variability of the original data. The plot of PC scores is shown in Fig. 7A. As can be seen, there are four distinct clusters of points. On the right side of the plot, aqueous phases and water can be found. Organic phases of the products and feeds are situated on the left side of the plot. Moreover, the variable chemical composition of the organic products was confirmed by moving position of the points from the top to the bottom of the plot. The most deoxygenated product is situated at the left bottom corner of the plot. On the other hand, the product treated using the mildest reaction conditions is the closest one to feeds. It follows, that while the PC1 is highly related to water content, PC2 is highly related to the carbonyl groups, aromatics and alkyl-aryl ethers.

To obtain more insight in the composition of the targeted organic products, a separate PCA model was built just for the organic products and feeds (Fig. 7B). The first two principal components (PC1 and PC2) captured 99.1% of the variability of the spectra. Since the variability caused by the large differences between the organic and aqueous phases (and water) was eliminated, *i.e.*, a new model without water and aqueous phases spectra was built, other spectral features became more important. Although the new first principal component is still related to the water content, the effect of the carbonyl groups, aromatics, alkyl-aryl ethers and other compounds increased. On the other side, the PC2 is positively correlated, *inter alia*, with the content of methylene groups. Nevertheless, since the PC2 is also positively correlated to the other types of compounds (*e.g.* glycosides) and the signal intensities of the methylene groups are influenced by the other bands, PC2 score values of the products do not have just an increasing trend. In other words, decreasing content of glycosides (and other compounds) prevailed the influence of the increasing methylene group content which caused that PC2 score values of the products obtained at the lowest temperatures have decreasing trend. As can be seen in the Fig. 7B, the products

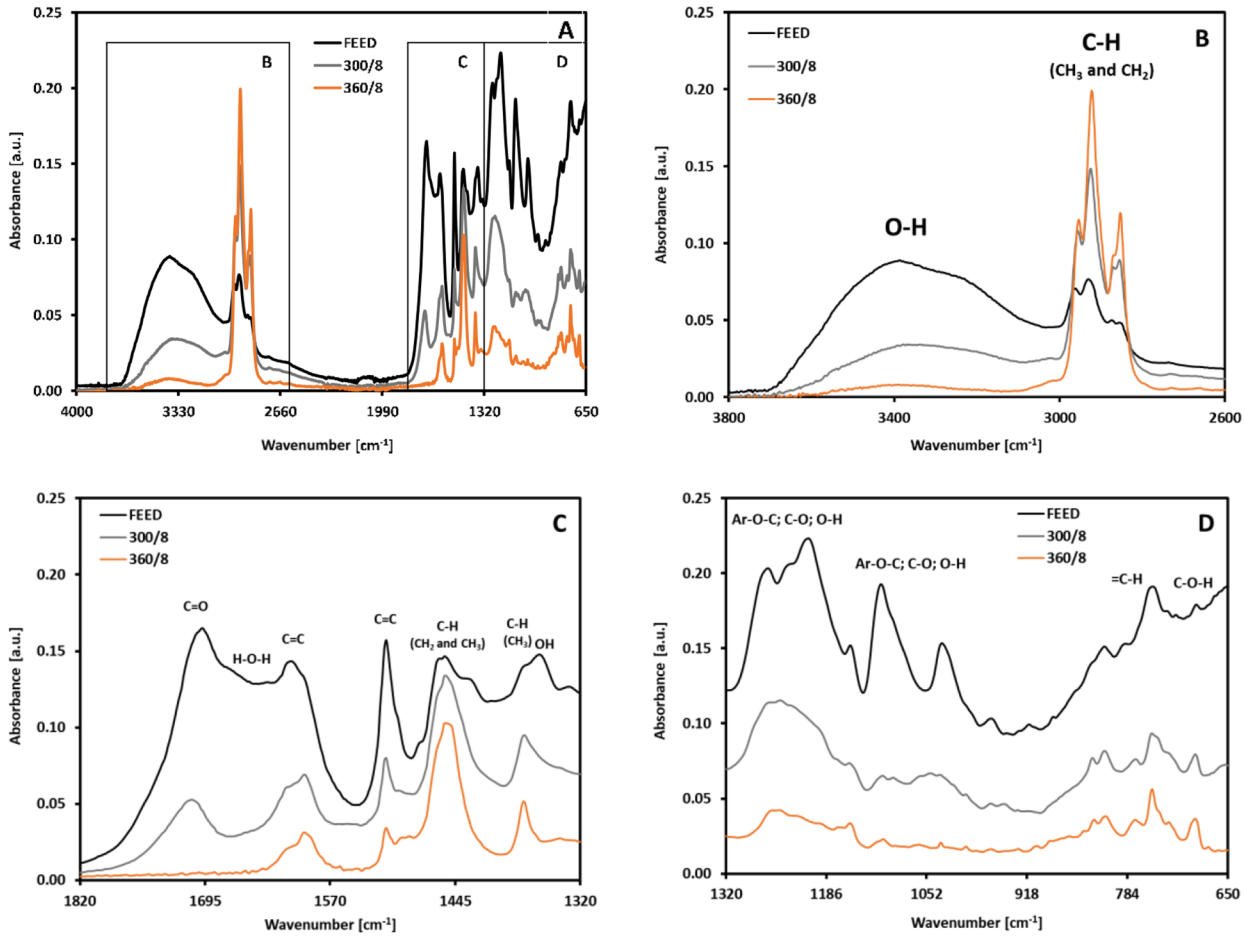


Fig. 6. Entire FTIR-ATR spectra (A), spectral region 3800–2600 cm^{-1} (B), spectral region 1820–1320 cm^{-1} (C) and spectral region 1320–650 cm^{-1} (D) of the feed and two products of the catalytic hydrotreating of the bio-oil.

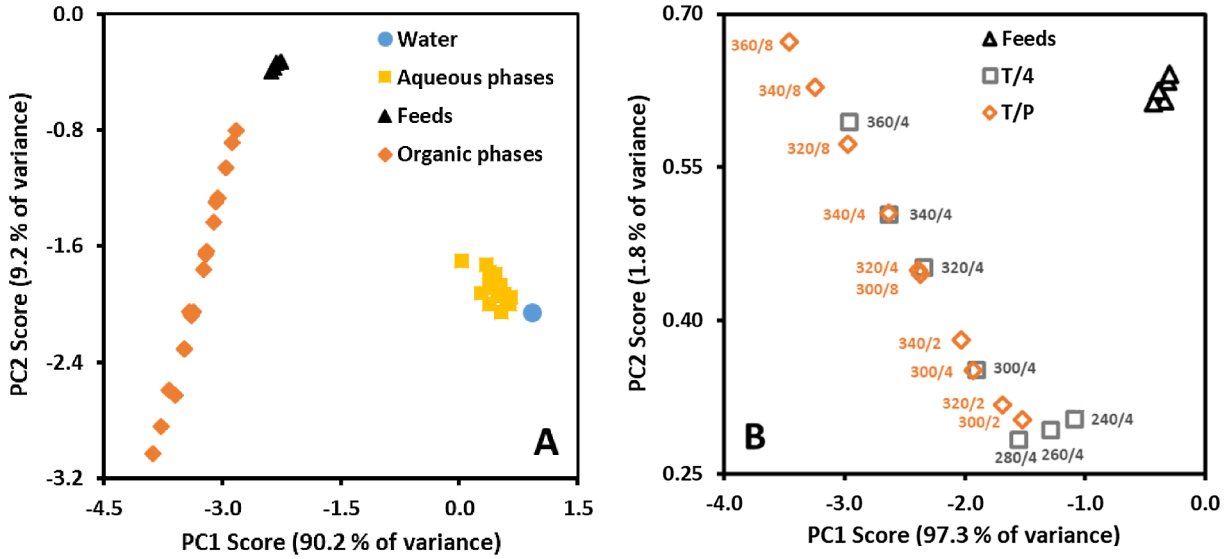


Fig. 7. PCA score plot (PC1 vs. PC2) of feeds, organic and aqueous phases and water (A) and of the organic phases of the products (denoted by T/P, *i.e.*, reaction temperature/reaction pressure) and feeds (B).

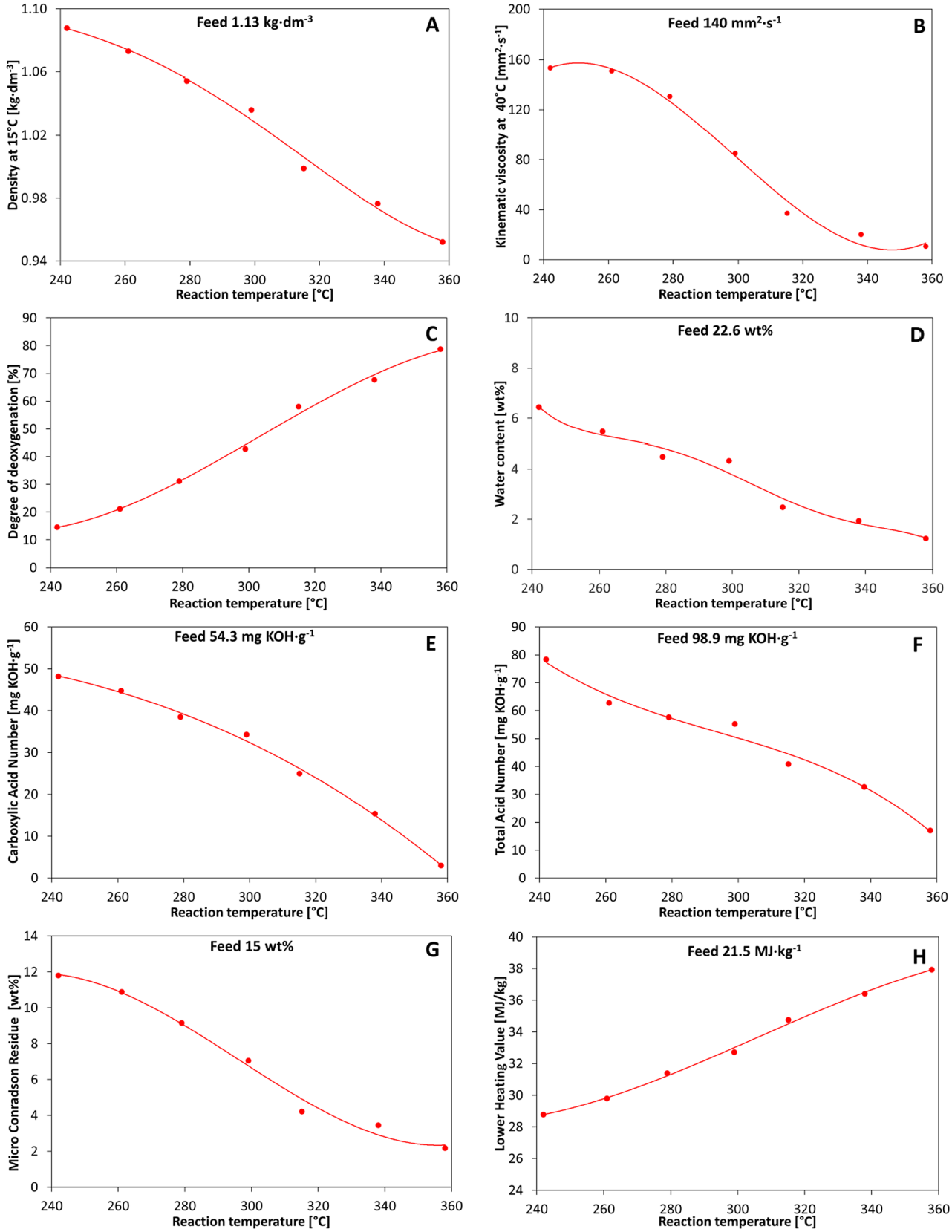


Fig. 8. Effect of temperature on physico-chemical properties of organic phase of products: density (A), kinematic viscosity (B), degree of deoxygenation, (DOD) (C), water content (D), carboxylic acid number (CAN) (E), total acid number (TAN) (F), micro Conradson carbonization residue (MCR) (G), lower heating value (H) at 4 MPa.

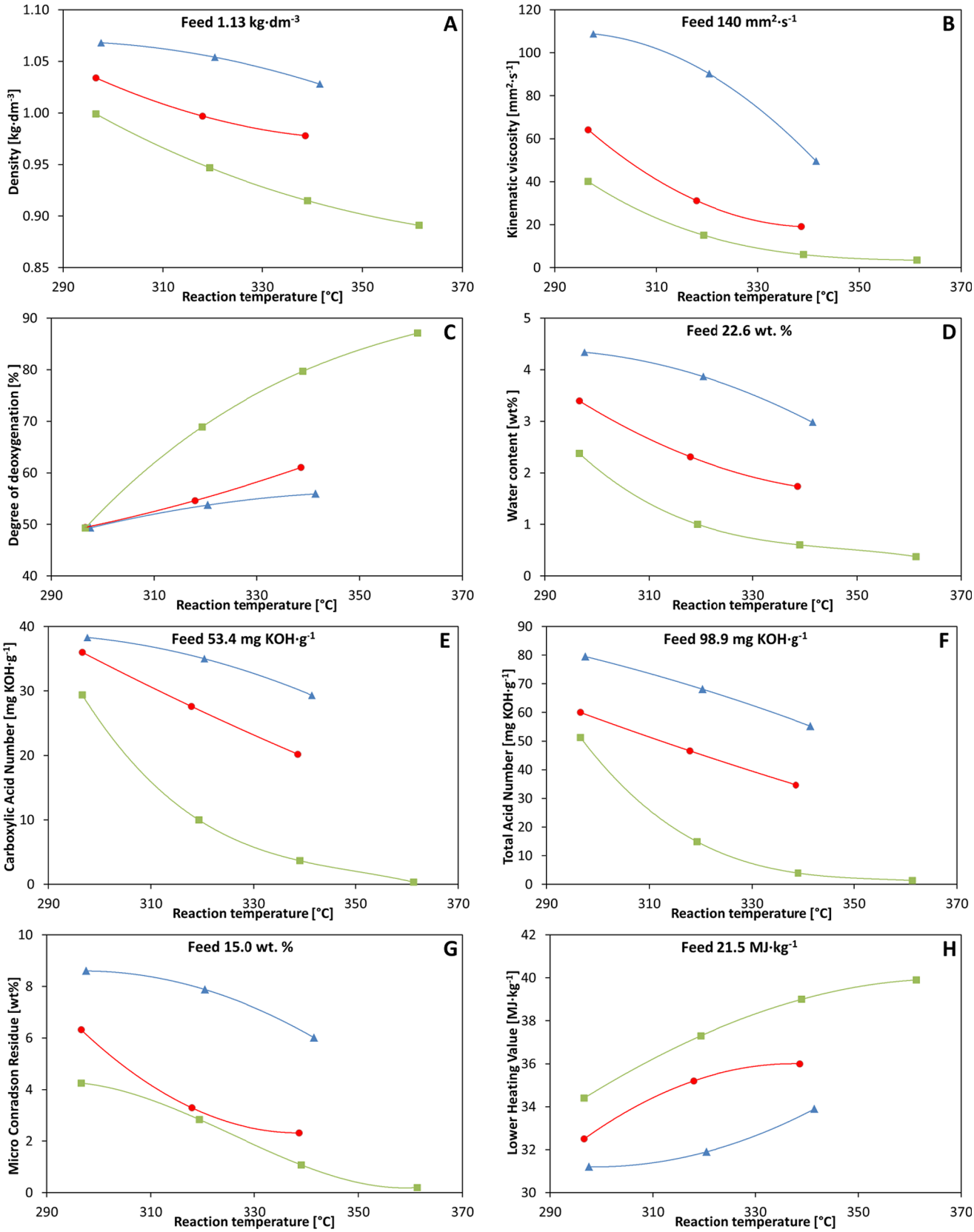


Fig. 9. Effect of temperature and pressure on physico-chemical properties of organic phase of products: density (A), kinematic viscosity (B), degree of deoxygenation (DOD) (C), water content (D), carboxylic acid number (CAN) (E), total acid number (TAN) (F), micro Conradson carbonization residue (MCR) (G), lower heating value (H); blue triangle – 2 MPa, red circle – 4 MPa, green square – 8 MPa. (For interpretation of the references to colour in this figure legend, the reader is referred to the web version of this article.)

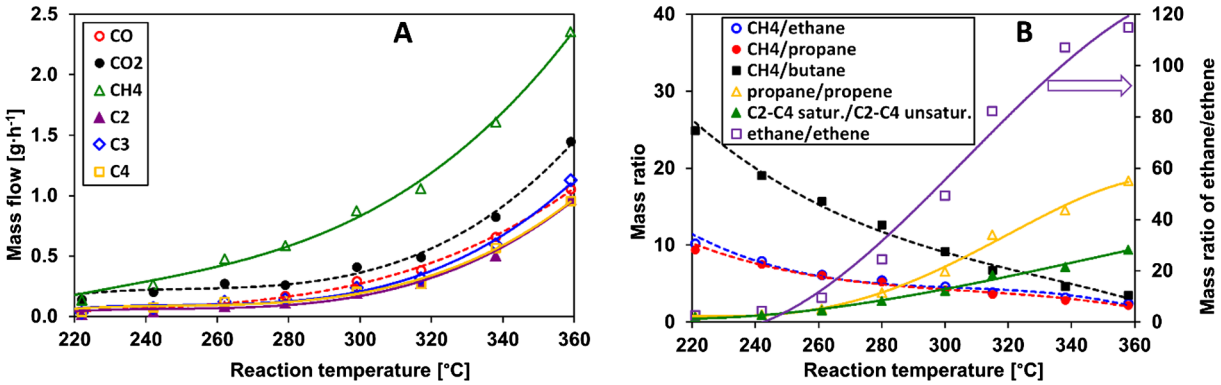


Fig. 10. Mass flow of gaseous products from bio-oil hydrotreating as a function of reaction temperature at 4 MPa (A) and selected concentration ratios (B).

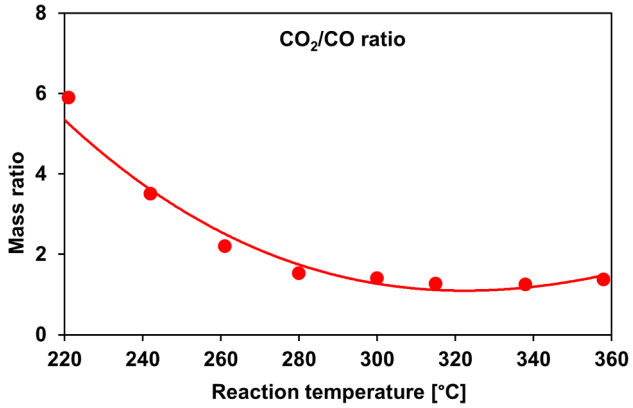


Fig. 11. Ratio CO/CO_2 in gaseous products as a function of reaction temperature at 4 MPa.

obtained in different experiments but using the same process conditions are situated very close to each other.

The results of the principal component analysis applied to the FTIR spectra of bio-oil and hydrotreated products clearly demonstrate that the method allows assessing rapidly the character of the products. This feature can be used to control the bio-oil hydrotreating by adjusting the hydrotreating process conditions to produce organic products having desired properties.

4.3. Properties of organic phases from hydrotreating

The changes in the properties of the hydrotreated products due to the increase in reaction temperature at 4 MPa are rather straightforward (Fig. 8). The increase in temperature resulted in a gradual decrease in density, kinematic viscosity, acid numbers, propensity to coking (expressed by the value of micro Conradson carbon residue, MCR) and water content. In line with the changes in elemental

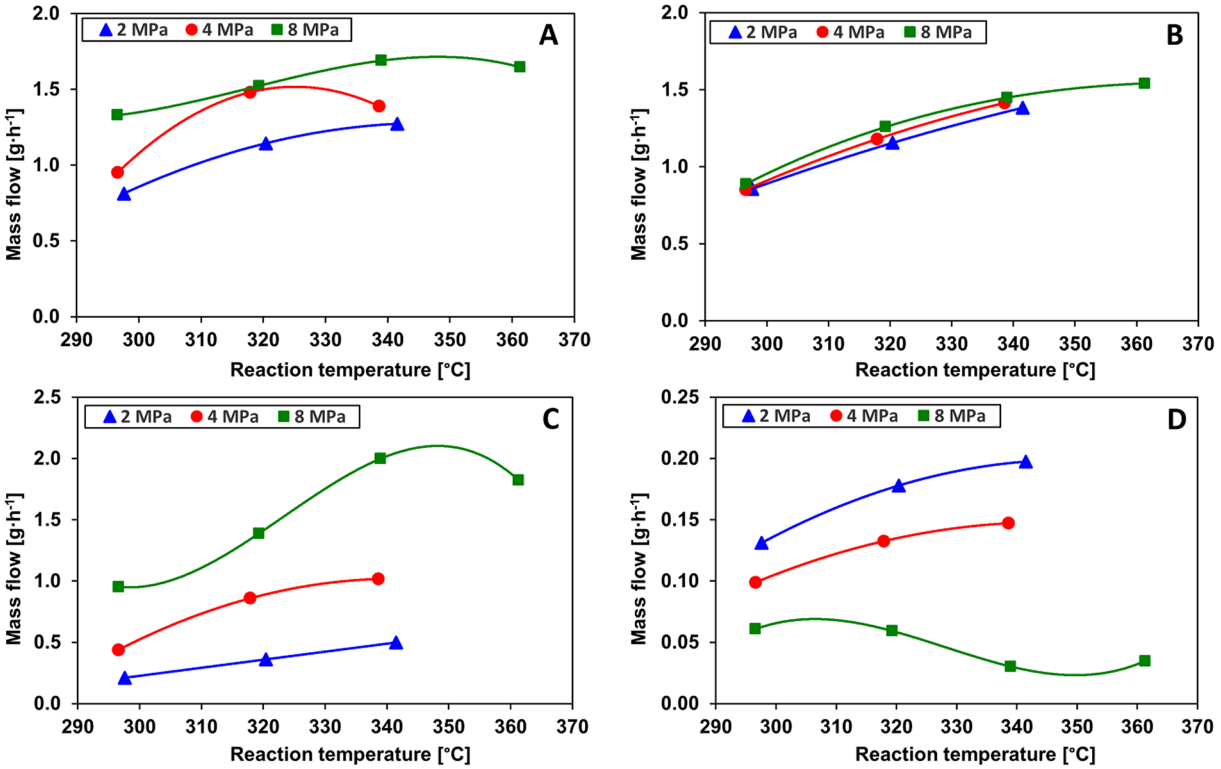


Fig. 12. Mass flow of gaseous products from bio-oil hydrotreating at different temperatures and hydrogen pressures – methane (A), CO and CO_2 (B), saturated C_2–C_4 (C) and unsaturated C_2–C_4 (D).

composition, degree of deoxygenation (DOD) and the lower heating value (LHV) increased with the increase in reaction temperature (Fig. 8). Analogous behaviour can be observed also for the set of experiments carried out over a wider range of hydrogen pressures (Fig. 9). As expected, deeper hydrogenation and deoxygenation observed at higher hydrogen pressure was reflected by a more pronounced decrease in the values of density, kinematic viscosity, acid numbers (TAN and CAN), MCR and water content. More interesting are, however, the different profiles characterizing the changes in the properties of hydrotreated products as a function of the reaction temperature.

All analysed properties change almost linearly over the studied range of temperature, LHV increases while other properties decrease. The changes in acid numbers (Fig. 8E and F), *i.e.* carboxylic and total acid number, disclose information about the type of acidic oxygenates present as well as about the extent of deoxygenation of these compounds. Whereas carboxylic acid number provides information about the concentration of carboxylic acids, the total acid number informs not only about the presence of carboxylic acids, but also about other acidic oxygenates, such as phenolics. At temperatures < 260 °C, the decrease in a CAN is slower than the decrease in TAN suggesting thus that other acidic organic compounds than carboxylic acids are predominantly hydrogenated in this range. The difference between TAN and CAN dropped from ca. 44 $mg{\cdot}g^{-1}$ obtained for the feed to about 18 $mg{\cdot}g^{-1}$ found at 260 °C (Fig. 8E and F). The difference remained constant while the temperature was increased from 260 to 340 °C, suggesting that in this range the observed deoxygenation was driven mainly by deoxygenation of carboxylic acids either by hydrodeoxygenation or decarboxylation. Finally, at 360 °C, the CAN was only 3 $mg{\cdot}g^{-1}$ and the difference between TAN and CAN decreased to 14 $mg{\cdot}g^{-1}$ indicating that also deoxygenation of some of the phenolics took place at the highest temperature. Nonetheless, it has to be kept in mind that phenol and some of the acids could have been extracted in the aqueous phase. The difference between TAN and CAN was also affected by the reaction pressure (Figs. 9E and 7F). Whereas at 2 MPa, the difference between TAN and CAN is 26 $mg{\cdot}g^{-1}$ at 340 °C or higher at lower temperatures, which is in line with the limited extent of deoxygenation reactions, at 8 MPa, the difference between TAN and CAN dropped to less than 5 $mg{\cdot}g^{-1}$ in the temperature range 320–360 °C, which proves that apart from carboxylic acids also other oxygenates, such as phenolics, were deoxygenated. Also, the TAN dropped to < 1.5 mg $KOH{\cdot}g^{-1}$, *i.e.* to < 2% of the original acidity, showing that the acidic compounds can be virtually completely removed under these conditions (*i.e.* at 360 °C and 8 MPa).

Keeping in mind the envisioned co-processing of the partially deoxygenated bio-oil with conventional refinery streams in a refinery, a simple preliminary blending test was carried out by blending the organic phases of the hydrotreated bio-oil products with straight run gas-oil (SRGO). Among the hydrotreated bio-oil products obtained here, only the organic phase of the product obtained at 360 °C and 8 MPa was fully miscible with the SRGO.

4.4. Gaseous products

The composition of gaseous products is an additional indicator that reflects the reactions that occur in the liquid phase. The changes in the concentration of gaseous products clearly show that there were virtually no cracking and/or hydrogenolytic reactions involving carbon-carbon bonds below 260 °C (Fig. 10a). An appreciable formation of gaseous products started only when reaction temperature exceeded 280 °C (Fig. 10A). Methane was the most abundant gaseous product formed by hydrogenolysis of methoxy compounds and by hydrogenation of carbon oxides (CO and CO_2) that were produced by decarboxylation and decarbonylation reactions. Altogether, C_1 gases constitute the majority of gaseous products, which supports the interpretation of the observed changes in the acid numbers as discussed above. The formation of C_1 gases was accompanied by the formation of C_2–C_4 hydrocarbons that originate from cracking reactions of larger molecules and from deoxygenation of short-chain alcohols, aldehydes, ketones and acids. In addition, several oxygenates were identified in the gas phase as well including acetone, methylacetate, butanone, methylfuran and dimethylfuran. Their concentrations were, however, low amounting to several tens to a few hundred mg/m^3.

A closer inspection of the gas phase composition reveals (Fig. 10B) that the relative share of particularly ethane and propane increases at the expense of methane (the concentration ratio of methane to ethane or propane drops from ca. 12 to about 2) confirming thus the importance of cracking and deoxygenation reactions at higher reaction temperatures. At the same time, the hydrogenation of alkenes is significantly favoured at higher reaction temperatures, as, *e.g.* the ethane-to-ethene ratio increased from about 2 to > 100 (Fig. 10B). It is also noteworthy that the CO_2/CO ratio decreased from 3.5 at 240 °C to ca. 1.4, a value that was constant in the range 280–360 °C (Fig. 11).

The composition of gaseous products obtained at 2–8 MPa and 300–360 °C is reported in Fig. 12. In line with the above-discussed results, the increase in reaction temperature resulted in the enhanced formation of all gaseous products but the differences between 320 and 340 °C were not very significant. It can be also seen (Fig. 12) that the formation of all products except alkenes is enhanced by higher hydrogen pressure. Again, this is in agreement with the observed deeper deoxygenation particularly at 8 MPa (Fig. 9C) resulting in more pronounced hydrogenolytic and deoxygenation activity of the catalyst.

5. Conclusions

The effect of reaction conditions on the composition and properties of products obtained by hydrotreating of bio-oil originating from ablative fast pyrolysis of straw was studied over a commercial sulphided $NiMo/Al_2O_3$ catalyst in a fixed bed reactor. The effect of temperature and hydrogen pressure was investigated in the range 240–360 °C and 2–8 MPa, respectively. The experiments have shown that the degree of deoxygenation increased and the properties of the products were improved with the increasing hydrotreating severity. In particular, the acidity expressed by total and carboxylic acid number (TAN and CAN) decreased to less than 2 mg $KOH{\cdot}g^{-1}$ and water content dropped to less than 1 wt% in products obtained at 360 °C and 8 MPa. This would allow processing of the products obtained by hydrotreating of straw-based bio-oil in a conventional refinery. At the same time, these products contained > 85% of the initial bio-oil energy content.

Considering the complex composition of bio-oil and products of its hydrotreating, it is important to be able to characterize their overall quality in a simple yet reliable way. Therefore, two methods were proposed and verified in this study. The first one is based on simulated distillation (SIMDIS) method and allows estimating the degree of deoxygenation relying on the different response of oxygenated and non-oxygenated compounds in this chromatographic technique. The second method is based on the principal component analysis (PCA) of the infrared spectra of bio-oils and products of their hydrotreatment. The method allows classify the products according to their structural composition that is accented by the PCA method. Consequently, the depth of hydrotreatment can be estimated reliably within a few minutes.

Acknowledgements

The results were obtained in the BioMates project. This project has received funding from the European Union's Horizon 2020 research and innovation program under grant agreement no. 727463. The publication reflects only the authors' view and the Commission is not responsible for any use that may be made of the information it contains. The authors are grateful to Tim Schulzke and Stefan Conrad (Fraunhofer UMSICHT) for providing the straw bio-oil used in the hydrotreating experiments.

References

[1] REN21. Renewables 2016 Global Status Report. Paris: REN21 Secretariat; 2016.
[2] Venderbosch RH, Ardiyanti AR, Wildschut J, Oasmaa A, Heeres HJ. Stabilization of biomass-derived pyrolysis oils. J Chem Technol Biotechnol 2010;85:674–86.
[3] REDII; Available from: https://eur-lex.europa.eu/legal-content/CS/ALL/?uri=CELEX%3A52016PC0767R%2801%29.
[4] Abbasi T, Abbasi SA. Biomass energy and the environmental impacts associated with its production and utilization. Renew Sustain Energy Rev 2010;14(3):919–37.
[5] Conrad S, Apfelbacher A, Schulzke T. Fractionated condensation of pyrolysis vapours from ablative flash pyrolysis. In: Hamburg, Germany Proceedings of 22rd European Biomass Conference & Exhibition (June 23rd–26th 2014). 2014:1127–33.
[6] Peacocke G, Bridgwater A. Ablative plate pyrolysis of biomass for liquids. Biomass Bioenergy 1994;7(1–6):147–54.
[7] Bridgwater AV. Review of fast pyrolysis of biomass and product upgrading. Biomass Bioenergy 2012;38:68–94.
[8] Lee H, Kim Y-M, Lee I-G, Jeon J-K, Jung S-C, Chung JD, et al. Recent advances in the catalytic hydrodeoxygenation of bio-oil. Korean J Chem Eng 2016;33(12):3299–315.
[9] Białek M, Gross-Gołacka E, Kaliski M. Rationalization process in the refining sector of the European Union in the context of activities aimed at restoring the competitiveness of refineries. AGH Drilling Oil, Gas 2014;31(1).
[10] Mortensen PM, Grunwaldt JD, Jensen PA, Knudsen KG, Jensen AD. A review of catalytic upgrading of bio-oil to engine fuels. Appl Catal A 2011;407:1–19.
[11] Wildschut J, Mahfud FH, Venderbosch RH, Heeres HJ. Hydrotreatment of fast pyrolysis oil using heterogeneous noble-metal catalyst. Ind Eng Chem Res 2009;48:10324–34.
[12] Baldauf W, Balfanz U, Rupp M. Upgrading of flash pyrolysis oil and utilization in refineries. Biomass Bioenergy 1994;7:237–44.
[13] Ly HV, Im K, Go Y, Galiwango E, Kim S-S, Kim J, et al. Spray pyrolysis synthesis of γ-Al_2O_3 supported metal and metal phosphide catalysts and their activity in the hydrodeoxygenation of a bio-oil model compound. Energy Convers Manage 2016;127:545–53.
[14] Rodríguez-Aguado E, Infantes-Molina A, Ballesteros-Plata D, Cecilia J, Barroso-Martín I, Rodríguez-Castellón E. Ni and Fe mixed phosphides catalysts for O-removal of a bio-oil model molecule from lignocellulosic biomass. Mol Catal 2017;437:130–9.
[15] Olarte MV, Padmaperuma AB, Ferrell JR, Christensen ED, Hallen RT, Lucke RB, et al. Characterization of upgraded fast pyrolysis oak oil distillate fractions from sulfided and non-sulfided catalytic hydrotreating. Fuel 2017;202(Supplement C):620–30.
[16] Mahfud FH. Exploratory studies on fast pyrolysis oil upgrading Ph.D. Wiskunde en Natuurwetenschappen, Rijksuniversiteit Groningen; 2007. p. 158.
[17] Mercader FDM, Koehorst PJJ, Heeres HJ, Kersten SRA, Hogendoorn JA. Competition between hydrotreating and polymerization reactions during pyrolysis oil hydrodeoxygenation. Am Instit Chem Eng J 2011;57:3160–70.
[18] Zanuttini M, Lago C, Querini C, Peralta M. Deoxygenation of m-cresol on Pt/γ-Al 2 O 3 catalysts. Catal Today 2013;213:9–17.
[19] Griffin MB, Baddour FG, Habas SE, Nash CP, Ruddy DA, Schaidle JA. An investigation into support cooperativity for the deoxygenation of guaiacol over nanoparticle Ni and Rh Catalysis. Sci Technol 2017;2:P.
[20] Echeandia S, Pawelec B, Barrio V, Arias P, Cambra J, Loricera C, et al. Enhancement of phenol hydrodeoxygenation over Pd catalysts supported on mixed HY zeolite and Al_2O_3. An approach to O-removal from bio-oils. Fuel 2014;117:1061–73.
[21] Elliott DC, Hart TR, Neuenschwander GG, Rotness LJ, Zacher AH. Catalytic hydroprocessing of biomass fast pyrolysis bio-oil to produce hydrocarbon products. Am Instit Chem Eng J 2009;28:441–9.
[22] Wildschut J. Pyrolysis oil upgrading to transportation fuels by catalytic hydrotreatment Ph.D Wiskunde en Natuurwetenschappen, Rijksuniversiteit Groningen; 2009. p. 190.
[23] French RJ, Stunkel J, Black S, Myers M, Yung MM, Iisa K. Evaluate impact of catalyst type on oil yield and hydrogen consumption from mild hydrotreating. Energy Fuels 2014;28:3086–95.
[24] Steele PH, Gajjela S, Yu F, Hassan E, Gresham G. Hydrocarbon production via biomas pyrolysis and hydrodeoxygenation. NSTI-Nanotech; 2009. p. 3.
[25] Novel Guo C. Carbon-supported transition metal phosphide catalysts for hydrodeoxygenation of fast pyrolysis oil MSc The University of Western Ontario; 2015. p. 128.
[26] Lup ANK, Abnisa F, Daud WMAW, Aroua MK. A review on reaction mechanisms of metal-catalyzed deoxygenation process in bio-oil model compounds. Appl Catal A: General 2017.
[27] Boullosa-Eiras S, Lødeng R, Bergem H, Stöcker M, Hannevold L, Blekkan EA. Catalytic hydrodeoxygenation (HDO) of phenol over supported molybdenum carbide, nitride, phosphide and oxide catalysts. Catal Today 2014;223:44–53.
[28] Zhao H, Li D, Bui P, Oyama S. Hydrodeoxygenation of guaiacol as model compound for pyrolysis oil on transition metal phosphide hydroprocessing catalysts. Appl Catal A 2011;391(1):305–10.
[29] Romero Y, Richard F, Brunet S. Hydrodeoxygenation of 2-ethylphenol as a model compound of bio-crude over sulfided Mo-based catalysts: promoting effect and reaction mechanism. Appl Catal B 2010;98(3):213–23.
[30] Patel M, Kumar A. Production of renewable diesel through the hydroprocessing of lignocellulosic biomass-derived bio-oil: a review. Renew Sustain Energy Rev 2016;58:1293–307.
[31] Ardiyanti AR, Khromova SA, Venderbosch RH, Yakovlev VA, Melián-Cabrera I, Heeres HJ. Catalytic hydrotreatment of fast pyrolysis oil using bimetallic Ni–Cu catalysts on various supports. Appl Catal A 2012;449:121–30.
[32] Mercader FDM, Groneveld MJ, Kersten SRA, Way NWJ, Schaverien CJ, Hogendoorn JA. Production of advanced biofuels: co-processing of upgraded pyrolysis oil in standard refinery units. Appl Catal A 2010;96:57–66.
[33] Yoshimura Y, Sato T, Shimada H, Matsubayashi N, Nishijima A. Influences of oxygen-containing substances on deactivation of sulfided molybdate catalysts. Appl Catal 1991;73(1):55–63.
[34] Laurent E, Delmon B. Influence of water in the deactivation of a sulfided NiMo/y-AI_2O_3 catalyst during hydrodeoxygenation. J Catal 1994;146:281–91.
[35] Gholizadeh M, Gunawan R, Hu X, de Miguel Mercader F, Westerhof R, Chaitwat W, et al. Effects of temperature on the hydrotreatment behaviour of pyrolysis bio-oil and coke formation in a continuous hydrotreatment reactor. Fuel Process Technol 2016;148:175–83.
[36] Horáček J, Kubička D. Bio-oil hydrotreating over conventional CoMo & NiMo catalysts: the role of reaction conditions and additives. Fuel 2017;198:49–57.
[37] Schulzke T, Conrad S, Westermeyer J. Ablative flash pyrolysis of straw – conversion process and valorization options for solid and liquid products. Biorefinery for food & fuels & materials. Montpellier, France; 2015.
[38] Christensen E, Ferrell J, Olarte MV, Padmaperuma AB, Lemmon T. Acid number determination of pyrolysis bio-oils using potentiometric titration. Report No: NREL/TP-5100-65890. Washington, DC: US Department of Energy; 2016.
[39] Næs T, Isaksson T, Fearn T, Davies T. A user friendly guide to multivariate calibration and classification. NIR Publications; 2002.
[40] Socrates G. Infrared and Raman characteristic group frequencies: tables and charts. John Wiley & Sons; 2001.